FINITE ELEMENT SIMULATION OF SHEAR SLITTING OF ALUMINUM WEBS

by

H. Lu, B. Wang, J. Ma, H. Viswanathan and M. Li
Oklahoma State University
USA

ABSTRACT

A three-dimensional finite element (FE) procedure has been developed to simulate shear slitting using ABAQUS/Explicit, and the process of shear slitting has been investigated for aluminum webs obeying elastic-plastic constitutive behavior. Shear failure criterion is used in the FE model to allow the creation of new surfaces as the blades guide the web separation. Shear slitting of aluminum webs is analyzed for different slitting parameters to determine their effects on the burr creation at a slit edge. The numerical study focuses on the effects of clearance and blade sharpness on burr formation. Numerical analysis has determined burr shape and burr height at slit edges. Burr profiles from FE simulation agree very well with those from experiments. The relations between burr height and clearance are also found from FE analysis. The mechanism of burr formation during shear slitting has been studied from numerical analysis. The relations between slitting parameters and burr height for different materials, determined from FE analysis, can potentially be used to determine the optimum shear slitting parameters for a given material.

INTRODUCTION

Shear slitting is a process to convert a web into two or more narrower webs using a pair of rotary engaged blades. In shear slitting operation, the quality of slit-edges is very important for many industrial applications. The ideal slit-edges should be smooth, clean free of debris, fines or hairs, and with minimum or no burr formation. This paper will focus on burr formation in shear slitting of aluminum webs. Burrs usually are formed as a result of the plastic flow in shear slitting and affect the edge quality of a web. The three-dimensional solution for an elastic-plastic web undergoing shear slitting is currently not available for the investigation of burr formation. Experimental investigations, such as our

previous work [1], have determined the relationship between burr height and slitting parameters for a few selected materials. However, for purpose of understanding the mechanism of shear slitting, numerical simulation using FE technique is a useful approach to model the shear slitting and burr formation process. There are very few published FE analysis results on shear slitting process. Due to some similarity between the metal cutting process and shear slitting, we list some references in metal cutting. Numerous researchers have carried out investigations of metal cutting, especially orthogonal cutting, using FE techniques. Klamecki [2] introduced the study of metal cutting using the finite element method. Later, Usui and Shirakashi [3] made a significant contribution to the development of FEM as the best predictive theory. Chip formation, cutting force, stress and strain distributions were predicted without any experimental input and numerical results agreed very well with experimental data. Recently, Park and Dornfeld [4-5] constructed a two dimensional model to investigate the burr formation in metal cutting using ABAQUS/Explicit [6]. Orthogonal metal cutting process is a two-dimensional problem and can be modeled as a plane strain problem if the cutting width is at least five times of the cutting thickness. As a result, the effect of exit angle, rake angle and backup material on burr formation has been studied based on FE results. So far, very few results are available in open literatures for web slitting investigation. It must be noted that despite some similarities between metal cutting (specifically shearing) and shear slitting, these two processes are fundamentally different. Orthogonal metal cutting is a two-dimensional problem while shear slitting is a three-dimensional problem. Viswanathan [7] has performed intensive two-dimensional FE analysis of shear slitting of aluminum webs, and reasonably good agreement on burr height between analysis and experiment has been reached. Welp and Wolf [8] carried out theoretical analysis of shear slitting of paper based on a three-dimensional material law and performed a two-dimensional FE analysis. On three-dimensional FE analysis of shear slitting process, Wisselink and Huetink proposed an Arbitrary Lagrangian Eulerian (ALE) formulation for the simulation of slitting in three-dimension [9]. The model is able to determine the shape of the sheared edge, and residual stresses in the strip for different slitting modes. But the crack front is not adapted during the calculation; the results thus depend for a great deal on the initial estimation of the crack front. The model can be improved with a procedure that adapts the position of the crack tip based on a fracture criterion. One major problem with this simulation is that simulated burr height does not compare well with experimental data. Therefore, there is a need to further understand the burr formation process and mechanism and to develop burr height predictive capability from three-dimensional simulation.

In this paper, a three-dimensional finite element procedure will be presented for the simulation of shear slitting process using ABAQUS/Explicit commercial code, and the effects of slitting parameters on burr formation will be investigated based on numerical simulation.

FE EXPLICIT DYNAMIC ANALYSIS

In this study, a commercial code ABAQUS/Explicit V6.2 [6] is used to carry out the numerical simulation of the shear slitting process. In the explicit dynamic finite element analysis, the governing equations of motion of the body are integrated using the explicit central difference integration rule:

$$\underline{\dot{u}}^{(i+1/2)} = \underline{\dot{u}}^{(i-1/2)} + \frac{\Delta t^{(i+1)} + \Delta t^{(i)}}{2} \underline{\ddot{u}}^{(i)} \tag{1}$$

and

$$\underline{u}^{(i+1)} = \underline{u}^{(i)} + \Delta t^{(i+1)} \underline{\dot{u}}^{(i+1/2)} \tag{2}$$

where the superscript i refers to the increment number, $\underline{u}$ represents the displacement vector, and Δt represents the time increment. The acceleration at the beginning of the increment is computed by

$$\underline{\ddot{u}} = [M]^{-1}(\overline{F} - \overline{I}) \tag{3}$$

where $[M]$ is the diagonal lumped mass matrix, $\overline{F}$ is the applied load vector, and $\overline{I}$ is the internal force vector.

The ductile failure with the shear failure option in ABAQUS/Explicit [5] is employed to simulate the shear slitting process. This allows the stable removal of failure elements from the mesh as a result of shearing, and/or tearing the web. Once a failure criterion is used, ABAQUS/Explicit automatically deletes elements from the mesh when the failure criterion is met in these elements. Failure is assumed to occur when the damage parameter ω exceeds 1. The damage parameter ω is defined as

$$\omega = \sum \left(\frac{\Delta \bar{\varepsilon}^{pl}}{\bar{\varepsilon}_f^{pl}} \right) \tag{4}$$

where $\Delta \bar{\varepsilon}^{pl}$ is an increment of the equivalent plastic strain, and $\bar{\varepsilon}_f^{pl}$ is the strain at failure.

THREE-DIMENSIONAL FINITE ELEMENT MODEL

To simulate the shear slitting of aluminum webs using 3-D FE model, part of web around two blades is taken as a deformable body and two blades are assumed as rigid bodies. The elastic-plastic properties of the web material (1050-H18), as shown in Table 1, are used to construct FE model. The stress and strain relation is in the piecewise relationship as input data in FE analysis. Rate dependence and thermal effects are neglected in the model.

Table 1: Mechanical properties of A1050-H18

UNIAXAIL TENSION TEST						
Thickness *mm*	Alloy	Dir.	*YS, MPa*	*UTS, MPa*	*% Elong.*	
					Unif.	*Tot.*
0.15	A1050-H18	*L*	159.85	169.49	1.4	2.5
		45	155.3	168.12	1.4	2.3
		T	162.6	177.07	1.4	2.0
0.29	A1050-H18	*L*	142.62	150.20	1.5	1.5
		45	142.62	152.96	1.5	1.5
		T	148.82	159.16	1.5	1.5

In Table 1, properties are given for 0.15 *mm* and 0.29 *mm* think webs. Material properties were given for three directions, which are length (*L*), transverse (*T*) and 45° direction with respect to the length direction. The difference in properties in different directions is small (up to 7%). We therefore assume an isotropic behavior in these webs. In Table 1, "YS" indicates yield stress, and "UTS" indicates ultimate tensile stress.

Since the web width/thickness and length/thickness ratios are rather large, this makes it difficult to model the actual long web. In the present FE model, the width and length of web are limited to a certain range within which the applying stress affects very intensely in order to reduce the total number of elements and save the computational time. The web in simulation has a thickness of 0.15 *mm*, a width of 2.4 *mm* and a length of 2 *mm*. The actual ratios of disk knife radius (90~92 *mm*) and web thickness (0.15~0.29 *mm*) are between 300 and 600. Since web thickness direction is the most important direction, in which the burr forms, the thickness of a web in simulation should be maintained. For this consideration, the circular upper and lower knives are modeled to be straight ones. The circular blade tip geometry is maintained to keep the model close to the actual situation. Blades in simulation are modeled as two connecting planes with the same relative

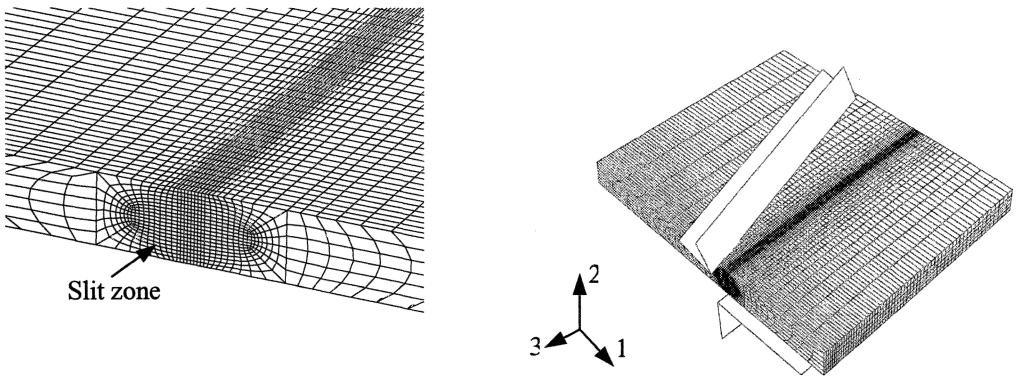

Fig. 1 (a) FE meshes of model (b) Assembly of components

position as in the actual blades in experiments. Fine meshes must be used for the web at the slitting zone because of stress concentration, and the mesh transition technique is used to mesh the web in the thickness-width plane to reduce the total amount of elements and degrees of freedoms. The FE meshes of model are shown in Fig. 1(a).

All three parts, the lower blade, the web and the upper blade, are assembled together as the actual case shown in Fig. 1(b). The lower blade is fixed in all directions at its reference point. The web is partially constrained at one corner for rigid displacements in all directions. The loads are applied by moving the upper blade toward the web and the bottom blade at a speed. To simulate the actual situation in experiments, the upper blade moves downward in direction 2 and rotates in negative 1 direction. The rest degrees of freedoms of the upper blade are constrained. Additionally, a pressure of $-10.3\ MPa$ is applied on web front and back surface to create a equivalent tensile stress in the web as in the experiment. Shear slitting involves the engagement of the blades and the web. In FE simulation, it can be modeled as a contact problem. The Coulomb friction with a coefficient 0.3 is used for the contact between blades and web in this model

FE SIMULATION AND RESULTS

Slitting Progress

Shear slitting process includes contact between blade and web at initial stage, followed by blade indentation, and finally web shearing and separation. These progresses are going on simultaneously and continuously at different points during steady shear slitting process. Burr is the out-of-plane plastic deformation formed during these progresses, which cannot be modeled in two-dimensional situation, and burr shape and height are related to the material failure mode. When the clearance is larger than the allowable clearance, the front bottom burr becomes thick and high. Fig. 2 is the slit edge at the clearance of $0.076\ mm$. Thick and high front bottom burr can be seen in the right side and rear top burr is shown in the left side from the bottom view.

Burr Profiles and Burr Heights

Slit edge section can be drawn from the steady state in 3D simulation since displacements at each node has been obtained. From FE analysis, the right side shows front bottom burr for the front slit edge and the left side is rear top burr for the rear slit edge. The burr profiles can be obtained from FE simulation. Fig.3 shows slit edge sections at 0.012 mm clearance for a web of 0.15 mm thick. The diagrams at the top of this figure are obtained from FE simulation and diagrams at the bottom are SEM micrographs of the slit edges. The two diagrams on the right are pictures for the front slit edges and the two diagrams on the left are pictures for the rear slit edges. It is seen that the burr profiles from FE simulation agree very well with those from experiment.

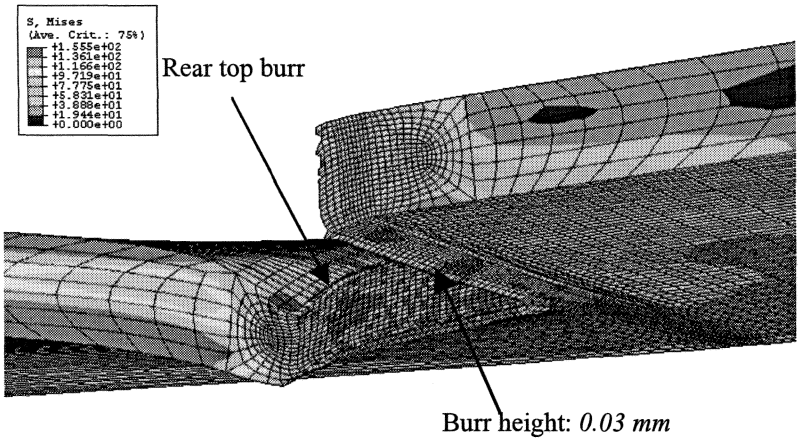

Fig. 2: Bottom view of slit edges

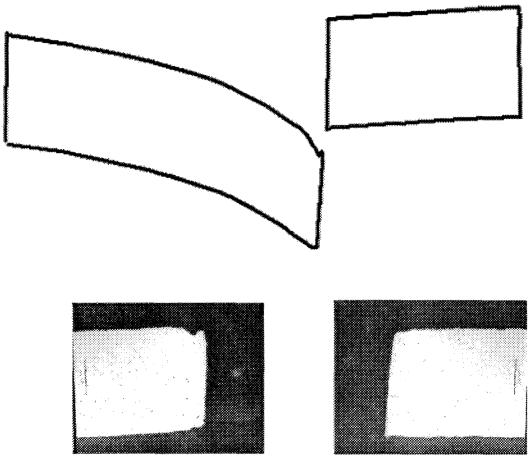

Fig. 3: Edge sections of small clearances

The effects of clearance on the burr height are plotted in Fig. 4 and Fig. 5. We can see the trend and magnitudes of burr height. Fig. 4 shows that there exists an allowable clearance for numerical simulation. Under the allowable clearance the front bottom burr height does not change much. But above the allowable clearance, the front bottom burr height increases drastically. Fig. 5 shows that the rear bottom burr almost keeps constant in burr height.

Burr profile and burr height have been obtained from FE simulation. We next use this FE simulation to investigate effects of burr height dependence on parameters not tested in experiments, such as blade sharpness.

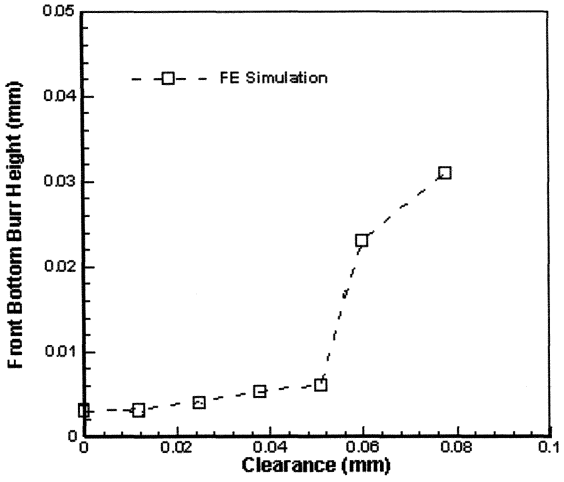

Fig. 4: Effect of clearance on front bottom burr

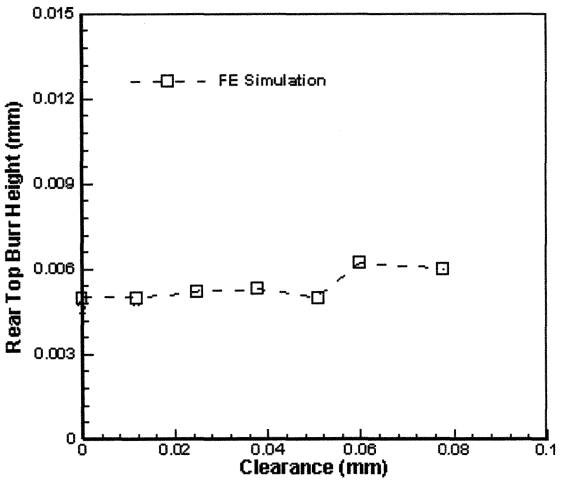

Fig. 5: Effects of clearance on rear top burr

Effects of Blade Sharpness

In punching of aluminum sheets [10], the cut surface roughness and the burr height increase when the blade becomes dull. In shear slitting, operators have the experience that slit quality becomes worse when the blade becomes dull. There is significant blade wear in traditional slitting. For the disk knife blade used in shear slitting at a speed of 500~800 m/min, it has to be replaced and sent to regrind in about one week, sometimes as short as one shift. There are times when the worn blades are used in shear slitting before the replacement of the blade. In all experimental investigation, only new and sharp blades are used. It is not appropriate to study the blade wearing under the current

laboratory slitter as the speed is too low. However it will be beneficial to understand how the blade sharpness affects the formation of burr through simulation. Blade sharpness is represented by the blade tip radius. A series of simulations were preformed with various blade tip radii while other slitting parameters were unchanged. Fig. 6 shows the edge sections from simulations with the same clearance but different blade radii. The arrows in this figure point to the major changes from the simulations.

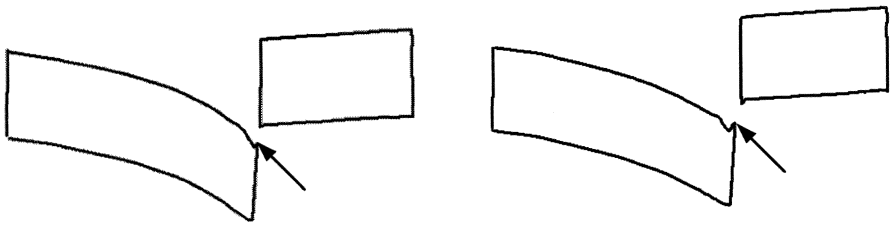

(a) *0.003 mm* blade radius (b) *0.018 mm* blade radius
Fig. 6: Slit edge profiles of different blade radii

Fig. 7 shows the burr height as a function of the blade radius from simulation. The web thickness is 0.15 mm and the clearance is *0.012 mm* in all these simulations. From Figs. 6 and 7 we can see that rear top burr has a stronger dependence on the blade sharpness/radius. The rear top burr height increases from *0.004 mm* to *0.105 mm*. And the front bottom burr increases from *0.003 mm* to *0.0048 mm* when the blade radius changes from *0.003 mm* to *0.018 mm*. It is not very sensitive to the blade radius as compared with the rear top burr.

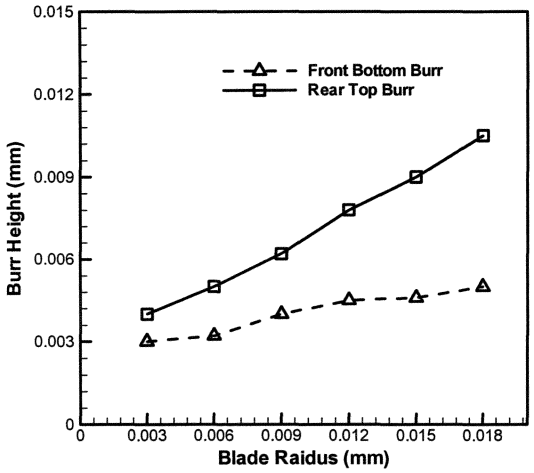

Fig. 7: Effects of blade radius on burr height

Burr Formation

Burrs are deformed in the web thickness-width plane that is perpendicular to the crack propagation direction. Study of stress distribution and deformation in this plane would lead to the understanding of burr formation. Fig. 8 shows the contour plots of in-plane shear stress for zero and large clearances at the initial engagement of the blade and the web plane. Before final separation, positive in-plane shear stresses are developed at the edges as shown in Fig. 8(b). The arrows point to the loci of the positive shear stresses. One positive shear stress zone is close to the top surface of the rear slit edge and the other one is close to the bottom surface of the front slit edge. These positive shear stress zones serve as pivot points for the development of burrs. The burrs formed in this situation are not high, close to the burr height at zero clearance at a zero rake angle. The rear top burr is formed only under this situation. The front bottom burr is also formed only in this same way when the clearance is smaller than the allowable clearance. It is noted that the positive shear stress is formed at the rear side before it is formed at the front side as shown in Fig. 9(a) & (b). Fig. 9 shows the magnified plot of contour level lines of the portion at earlier and later slitting stage of a web section. The magnitude of stress is labeled. If the pivoting positive shear stress zone stays longer, it results in higher burr height. Therefore, the rear top burr is higher than the front bottom burr when both burrs are formed due to the pivoting positive shear stress zones. The formation of the pivoting positive shear stress is inevitable in shear slitting at a zero rake angle.

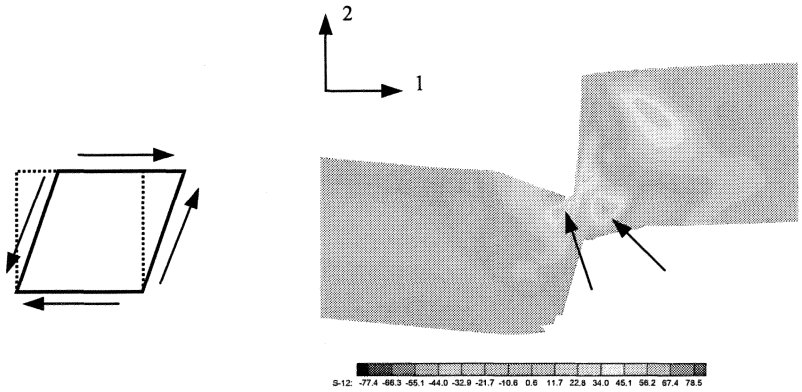

(a) Deformation of an element under positive shear stress
(b) Contours of positive shear stress under large clearance
Fig. 8: Development of positive shear stress in the slit zone

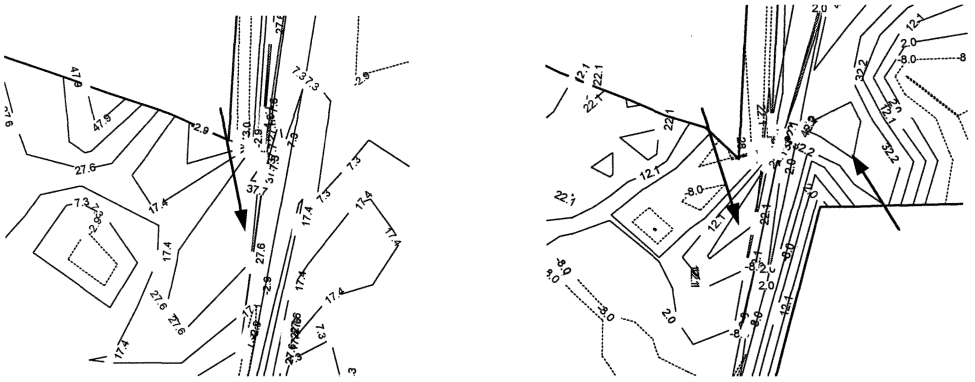

(a) Earlier slitting stage of a web section (b) Later slitting stage of a web section

Fig. 9: Contours of positive shear stress under small clearance

Under zero rake angle slitting, the formation of pivoting positive shear stress causes the formation of burrs. The existence of rake angle can cause the formation of the positive shear stress zones in the rear edge to a very later stage. In Fig. 10, there is no pivoting positive shear stress in the rear slit edge in the left diagram. At final separation, some pivoting positive shear stress can be seen in the right diagram.

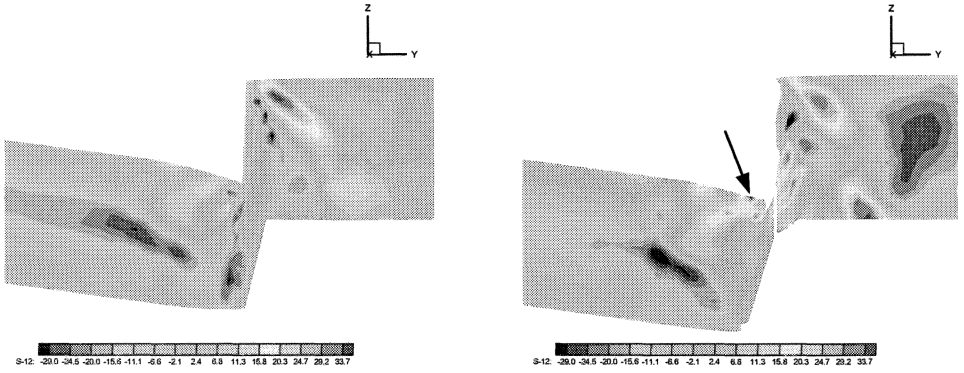

Fig. 10: Contour of shear stress under rake angle slitting

Blade indentation into to the also induce normal stress in the web. Normal stress is high in the slit area. Fig. 11 shows the distributions of normal stresses in the 1-1 direction for zero clearance and large clearance under zero rake angle. By comparison, we see that a large clearance induces high magnitude of normal stress.

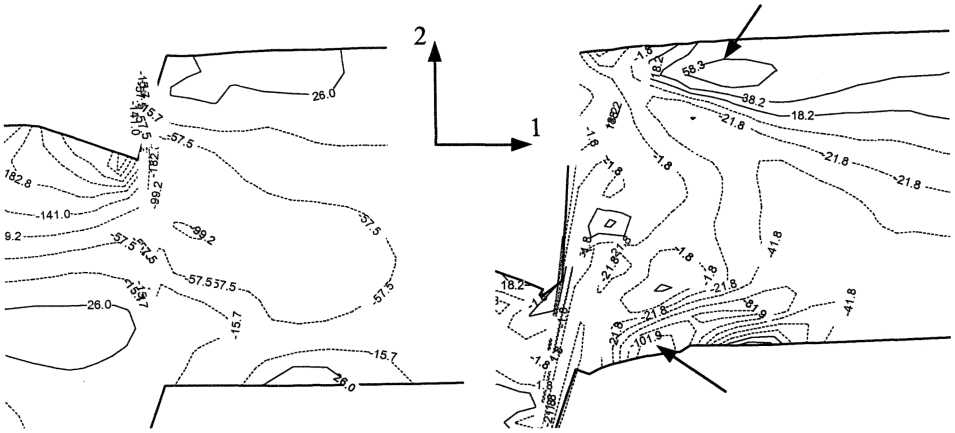

(a) Slitting at zero clearance (b) Slitting at 0.06 mm clearance

Fig. 11: Plot of normal stress at different clearances

When the clearance is greater than zero, the normal stress in the front slit edge is positive on the top and negative on the bottom as shown the right diagram in Fig. 11. It is noted that this moment is highly dependent on the clearance. When clearance is larger than the allowable clearance, significant bending moment is induced on the front slit edge by the blade movement as shown in Fig. 12(a). The effect of this moment can be seen from FE contour plot of the normal stress due to bending. This moment causes the front slit edge to deform like a cantilever. Moreover the upper blade moves downward to pull the material between the two blades to deform further resulting in a high and thick front bottom burr. The von Mises stress in this area, as shown in Fig. 12(b) indicated by an arrow, is higher than the yield strength of the material so that the front bottom burr is formed permanently. Therefore, when the clearance is larger than the allowable clearance, the front bottom burr is formed in two steps, the burr due to edge bending and the burr due to positive shear stress. When the clearance is smaller than the allowable clearance, von Mises stress in the slitting area is not high enough to cause plastic deformation.

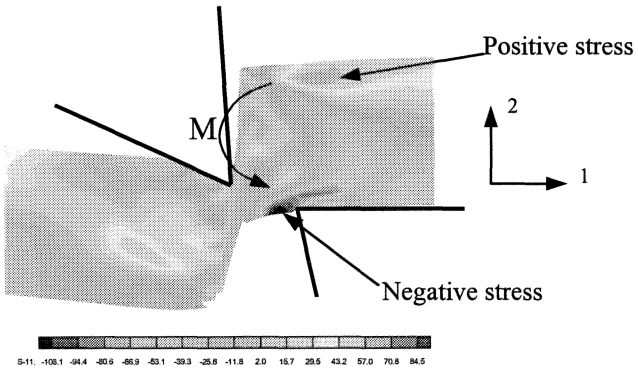

(a) Normal stress S_{11} contour under large clearance

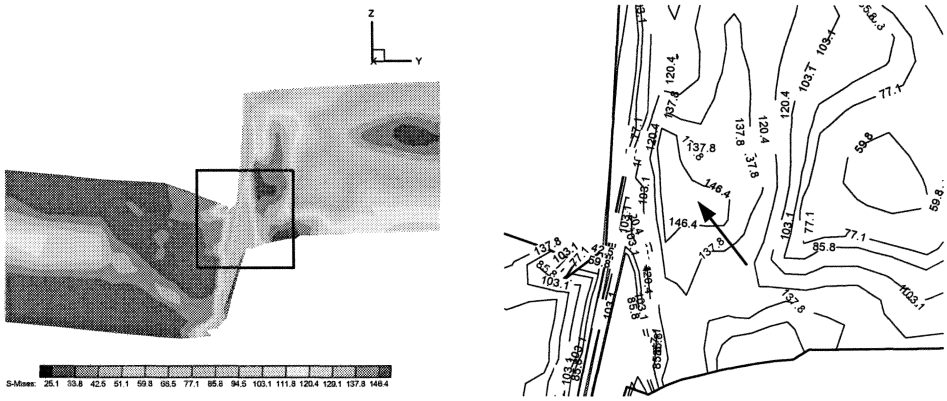

(b) von Mises stress contour under large clearance

Fig. 12: Formation of high and thick front bottom burr

The moment in the front slit edge has a strong dependence on the clearance. Fig. 13 is a plot of the moment as a function of clearance. We see a linear relation between the moment and the clearance when the clearance is less than 0.05mm (33% of the web thickness). There is an abrupt change of the moment, associated with instability in slitting, when the clearance increases from 0.05mm to 0.06mm (c/t from 0.33 to 0.4) as shown in Fig. 13. A sudden increase of the front bottom burr height occurs in this clearance range. We define a first dimensionless number c/t, the normalized clearance, where c is the clearance and t is the web thickness. The second dimensionless parameter is r/c, where c is the clearance and r is the blade radius. Larger r, indicating dull blade, results in a more diffuse plastic zone, thus larger burr height. It is noted that c/t and r/c are also important in punching of aluminum sheets [10]. We define a third dimensionless parameter, dimensionless moment, $\frac{M}{tr\sigma_y}$, where M is the moment on a unit depth section, t is the web thickness, r is the blade radius and σ_y is the yield strength of the material. This parameter characterizes the front bottom burr profile relative to web thickness and blade sharpness. A larger dimensionless moment causes instability in shear slitting, resulting in large front bottom burr height.

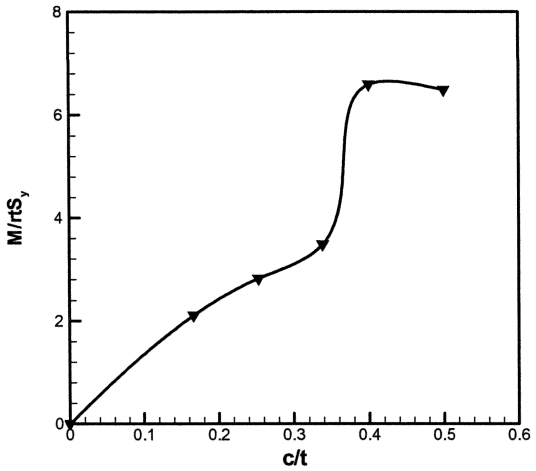

Fig. 13: Dimensionless moment as a function of nominal clearance

CONCLUSIONS

The finite element analysis on shear slitting process provides insight information on the mechanism of burr formation. FE simulations before experiment have been conducted so that some results can be used for optimization of appropriate slitting parameters for a given material. The effect of different clearances, blade sharpness/radius on burr formation has been simulated and new blade geometries, boundary conditions and webs with different materials can also be implemented in FE models. In explicit dynamic FE analysis, shear failure criterion was used to allow the creation of new surfaces in the web as the blades guided the web separation in the machine direction. The burr shape and burr height have been obtained from FE results. Burr profiles from FE simulation agree very well with those from experiments. Stress fields in a web section were studied to investigate the mechanisms of burr formation. It was found that burrs are formed after the formation of pivoting positive shear zones near the slit edge. When the clearance is larger than the allowable value, the moment in the front slit edge increases drastically; it is this moment that causes the front slit edge to deform similar to a cantilever. Therefore, it can be concluded that there exists an allowable clearance for limitation of burr heights during shear slitting process.

ACKNOWLEDGEMENTS

The authors acknowledge the support under grant # 9697-1 from the Web Handling Research Center at Oklahoma State University (OSU), sponsored by twenty companies that include 3M, Eastman Kodak, ALCOA, AET Packaging, Fife, Polaroid, Rockwell Automation, and Xerox, and the support from 3M Non-Tenured Faculty Grant, as well as the support from NSF under CMS-9872350 and CMS-9985060.

REFERENCES

1. Lu, H., Wang, B., and Iqbal, J., "Deformation in shear slitting of polymeric webs," Proceedings of the Sixth International Conference on Web Handling, Oklahoma, USA, June, 2001, pp. 389-402.

2. Klamecki, B.E. "Incipient Chip Formation in Metal Cutting—Three Dimensional Finite Element Analysis," Ph.D. dissertation, Univ. of Illinois Urbana-Champaign, 1973.

3. Usui, E. and Shirakashi, T., "Mechanics of Machining—From 'Descriptive' to 'Predictive' Theory," ASME Publication PED, 1982.

4. Park, I. W. and Dornfeld, D. A., "A study of burr formation processes using the finite element method: Part I," Journal of Engineering Materials and Technology, Vol. 122, 2000, pp. 221-228.

5. Park, I. W. and Dornfeld, D. A., "A study of burr formation processes using the finite element method: Part II-The influences of exit angle, rake angle, and backup material on burr formation processes," Journal of Engineering Materials and Technology, Vol. 122, 2000, pp. 229-237.

6. Hibbitt, Karlsson & Sorensen, Inc., ABAQUS/EXPLICIT User's Manual, 2001.

7. Viswanathan, H. "Exploratory Investigation of Shear and Score Slitting Using FEM And Edge Characterization of Slit Non-woven Web," Master's thesis, Oklahoma State University, 2001.

8. Welp, E. G. and Wolf, E., "Theoretical analysis of shear slitting of paper of the basis of a three-dimensional material law," Proc. of the Fifth International Conference on Web Handling, June 1999, pp. 217-233.

9. Wisselink, H.H. and Huetink, J., "Simulation of the slitting progress with the finite element method," Procedings of the SheMet'99, Sept. 27-28, 1999.

10. Li, M., "Micromechanisms of deformation and fracture in shearing aluminum alloy shear," International Journal of Mechanical Science, Vol. 42, 2000, pp. 907-923.